



HAL
open science

The insect attractant 1-Octen-3-ol is the natural ligand of bovine odorant-binding protein

Roberto Ramoni, Florence Vincent, Stefano Grolli, Virna Conti, Christian Malosse, Francois Boyer, Patricia Nagnan-Le Meillour, Silvia Spinelli, Christian Cambillau, Mariella Tegoni

► To cite this version:

Roberto Ramoni, Florence Vincent, Stefano Grolli, Virna Conti, Christian Malosse, et al.. The insect attractant 1-Octen-3-ol is the natural ligand of bovine odorant-binding protein. *Journal of Biological Chemistry*, 2001, 276 (10), pp.7150-7155. 10.1074/jbc.M010368200 . hal-02677183

HAL Id: hal-02677183

<https://hal.inrae.fr/hal-02677183>

Submitted on 31 May 2020

HAL is a multi-disciplinary open access archive for the deposit and dissemination of scientific research documents, whether they are published or not. The documents may come from teaching and research institutions in France or abroad, or from public or private research centers.

L'archive ouverte pluridisciplinaire **HAL**, est destinée au dépôt et à la diffusion de documents scientifiques de niveau recherche, publiés ou non, émanant des établissements d'enseignement et de recherche français ou étrangers, des laboratoires publics ou privés.

The Insect Attractant 1-Octen-3-ol Is the Natural Ligand of Bovine Odorant-binding Protein*

Received for publication, November 15, 2000, and in revised form, December 6, 2000
Published, JBC Papers in Press, December 12, 2000, DOI 10.1074/jbc.M010368200

Roberto Ramoni‡§, Florence Vincent¶, Stefano Grolli‡, Virna Conti‡, Christian Malosse||, François-Didier Boyer||, Patricia Nagnan-Le Meillour||, Silvia Spinelli¶, Christian Cambillau¶, and Mariella Tegoni¶**

From the ¶Architecture et Fonction des Macromolécules Biologiques, Unité Mixte de Recherche 6098, CNRS and Universités Aix-Marseille I and II, 31 Chemin Joseph Aiguier, 13402 Marseille Cedex 20, France, ‡Istituto di Biochimica Veterinaria, Facoltà di Medicina Veterinaria, Università di Parma, Via del Taglio 8, 43100 Parma, Italy, and ||Institut National de Recherche Agronomique, Unité de Phytopharmacie et des Médiateurs Chimiques, Route de Saint-Cyr, F-78026 Versailles Cedex, France

Bovine odorant-binding protein (bOBP) is a dimeric lipocalin present in large amounts in the respiratory and olfactory nasal mucosa. The structure of bOBP refined at 2.0-Å resolution revealed an elongated volume of electron density inside each buried cavity, indicating the presence of one (or several) naturally occurring copurified ligand(s) (Tegoni *et al.* (1996) *Nat. Struct. Biol.* 3, 863–867; Bianchet *et al.* (1996) *Nat. Struct. Biol.* 3, 934–939). In the present work, by combining mass spectrometry, x-ray crystallography (1.8-Å resolution), and fluorescence, it has been unambiguously established that natural bOBP contains the racemic form of 1-octen-3-ol. This volatile substance is a typical component of bovine breath and in general of odorous body emanations of humans and animals. The compound 1-octen-3-ol is also an extremely potent olfactory attractant for many insect species, including some parasite vectors like *Anopheles (Plasmodium)* or *Glossina (Trypanosoma)*. For the first time, a function can be assigned to an OBP, with a possible role of bOBP in the ecological relationships between bovine and insect species.

Several isoforms of odorant-binding protein (OBP)¹ have been purified and characterized from the nasal mucosa of many mammalian species (1–5). These 19-kDa soluble proteins are produced in large amounts in seromucous glands of the respiratory and olfactory epithelium and are secreted in the mucus that layers the surface of nasal mucosa (5). OBPs belong to the lipocalin family, which is composed of structurally related soluble proteins that bind different types of small hydrophobic molecules (6, 7). These proteins are usually monomeric and are formed of a nine-strand β -barrel and a C-terminal α -helix (6, 7). Bovine OBP is a dimer in which the C-terminal domain (resi-

dues 125–159) is swapped between the two monomers, a peculiar feature that seems to be specific to the bovine species (8, 9). An elongated volume of electron density was observed in each of the two internal buried cavities. In the 2.0-Å resolution electron density we assigned this electron density to an unknown molecule of 8–10 non-hydrogen atoms (8), whereas Bianchet *et al.* (9) tentatively assigned it to a terpenoid compound, citronellyl acetate. Several structures of lipocalins have revealed the presence of specific or nonspecific copurified ligand in their binding sites, such as retinol in retinol-binding protein (10) and pheromones in the major urinary protein (11). The structure of porcine OBP, instead, revealed an empty cavity (12).

The recent characterization of the binding properties of porcine OBP (pOBP) in solution and in the crystal (13) has established that a high degree of hydrophobicity coupled to a molecular mass between 160 and 200 daltons is the main requirement for a ligand to match the β -barrel cavities, independently of its odorous properties, chemical class, and molecular structure. Some of the ligands of pOBP have a very low olfactory threshold (13), whereas others, for instance the toxic 7–11 carbon alkyl aldehydes (14), cannot be considered real odorous compounds (15). The K_d values, obtained or estimated from direct and competitive equilibrium binding experiments, are in the micromolar range for most of the OBP ligands (1, 13–18). The peculiar binding properties of OBPs with respect to other lipocalins (low ligand specificity and low affinities) and the very high quantities of protein found in nasal epithelium have suggested that OBPs might function as odorant carriers and/or scavengers for olfactory receptors or that they might be involved in endogenous detoxification processes (19). In this latter hypothesis it has been proposed that OBPs might deliver, to the appropriate degradative pathways, some toxic compounds produced during nasal epithelium turnover and inflammatory processes in charge of the nasal mucosa (19). These two hypotheses are not mutually exclusive, and at present, no direct experimental evidence supports or excludes any of them. On the contrary, the present data suggest that the two functions might be carried out in parallel. In the present work, the unambiguous identification of the copurified natural ligand of bovine OBP as the insect attractant 1-octen-3-ol makes it possible to hypothesize a role for bOBP in the ecological relationships between bovine and several insect species.

MATERIALS AND METHODS

OBP Purification and Extraction of the Ligand—Single bovine nasal mucosa samples were collected during fall and winter from freshly slaughtered 16–18-month-old males of different geographical origins

* This work was supported in part by a BIOTECH contract from the European Union (BIO4–98-0420). The costs of publication of this article were defrayed in part by the payment of page charges. This article must therefore be hereby marked “advertisement” in accordance with 18 U.S.C. Section 1734 solely to indicate this fact.

The atomic coordinates and structure factors (code 1G85 and 1HN2) have been deposited in the Protein Data Bank, Research Collaboratory for Structural Bioinformatics, Rutgers University, New Brunswick, NJ (<http://www.rcsb.org/>).

§ To whom correspondence may be addressed. Tel.: 39-0521-90-27-67; Fax: 39-0521-90-27-70; E-mail: vetbioc@unipr.it.

** To whom correspondence may be addressed. Tel.: 33-491-164-512; Fax: 33-491-164-536; E-mail: tegoni@afmb.cnrs-mrs.fr.

¹ The abbreviations used are: OBP, odorant-binding protein; pOBP, porcine OBP; bOBP, bovine OBP; AMA, 1-aminoanthracene; GC/MS, gas chromatography/mass spectrometry.

(Northern Italy and France). OBP was purified according to the procedure previously reported by Bignetti *et al.* (20). Briefly, purification consists of an ammonium sulfate fractionation of the soluble proteins in the extract of nasal mucosa, followed by two rounds of fast protein liquid anion exchange chromatography (Baker bond and Mono-Q) and a final acidic step. The purity of the protein was checked by SDS-polyacrylamide gel electrophoresis, and its functionality was determined in binding tests with 1-aminoanthracene (AMA) as fluorescent probe (21–23). The molar absorption coefficient of 47,000 ($M^{-1} cm^{-1}$ /bOBP dimer) at 280 nm was determined according to the Edelhoc method (24) as described by Pace *et al.* (25). The natural ligand was extracted from samples of native and denatured OBP with different organic solvents (diethyl ether, methylene chloride, and hexane). The protein (a 7.0-mg/ml OBP solution in 20 mM Tris-HCl, pH 7.8) was previously denatured by overnight incubation at room temperature in the presence of 7.5 M urea. The ligand extraction was performed by vortexing mixtures of OBP-organic solvent in glass tubes (1:1 volumetric ratio), and the organic phases were analyzed by GC/MS. Aliquots of Tris buffer and Tris buffer containing 7.5 M urea were treated with the same extraction procedure, and the organic phases were analyzed by GC/MS as blanks.

GC/MS Identification and Chiral Determination—Analyses were conducted on a Varian Saturn II trap spectrometer coupled to a Varian 3400 gas chromatograph. Mass spectra were recorded in electronic impact mode, with a mass range of 40–300 atomic mass units. A 30-m, 0.32-mm internal dimension, 0.5- μm df RTX-5MS column (Restek, Bellefonte, PA) was used for analysis, and the program temperature was from 50 °C (1 min) to 280 °C at 10 °C/min with helium as carrier gas at 10 p.s.i. pressure. Samples were injected in a septum programmable injector heated at 250 °C. Chemical ionization was conducted on a Nermag R10–10C quadrupole mass spectrometer, with ammonia as reactant gas at 10^{-4} pressure in the source housing. Spectra were recorded with a mass range of 70–300 atomic mass units. The mass spectrometer was coupled to a Varian 3400 gas chromatograph equipped with a Ross injector heated at 240 °C and a similar column used with the same program temperature.

To determine the *R* or *S* configuration of the natural product, derivatization of standard and natural compound were conducted as follows. A solution of pyridine (50 mg/ml) in dry ether (15 μl) and a solution of *S*-lactyl chloride reagent (26) (25 mg/ml) in dry methylene chloride (30 μl) was added to a solution of standard commercially available 1-octen-3-ol (racemic or *R*-(-)) (50 ng) in hexane (30 μl) or natural extract in hexane (40 μl) placed in a micro-conic flask. Closed flasks were kept at room temperature for 30 min. The solution was then diluted with hexane (50 μl) and washed successively with water (50 μl), aqueous 5% sodium bicarbonate ($2 \times 50 \mu l$), and water (50 μl). The samples were directly analyzed by GC/MS. Four samples of bOBP coming from animals of different geographical origin yielded indistinguishable results.

Crystallization, Data Collection, and Refinement of Bovine OBP—OBP crystals were obtained by micro-dialysis of a 10 mg/ml protein solution against 28–32% ethanol, in 50 mM citrate, pH 5.4 at 4 °C. The crystals belong to the space group $P2_1$, with cell dimensions $a = 55.9 \text{ \AA}$, $b = 65.5 \text{ \AA}$, $c = 42.7 \text{ \AA}$, and $\beta = 98.8^\circ$, and contain one homodimer in the asymmetric unit. Data were collected on a Mar-research 345 image plate placed on a Rigaku RU2000 rotating anode. Data collection was performed at room temperature, because cryocooling always yielded data sets that could not be used in refinement. Indexation and integration were performed with DENZO (27); data scaling was performed with SCALA (28); and data reduction was performed by TRUNCATE (28) (see Table I). The bOBP-AMA complex was obtained by soaking the crystals in a synthetic crystallization solution containing 2 mM AMA overnight at 4 °C. Data collection, scaling, and reduction were performed as with native bOBP (see Table I).

The refinement of bovine OBP containing its natural ligand or AMA made use of the previously determined bOBP structure as a starting model (8; 1OBP). The atomic structure of 1-octen-3-ol and of AMA were built with the program TURBO-FRODO (29), and topology and force field data were defined in the suitable files of CNS (30) by the automated procedure XDICT (G.L. Kleywegt). The models were then refined using CNS version 1.0 (30). Cycles of refinement were alternated with manual refitting into sigmaA-weighted electron density maps (31) with the graphic program TURBO-FRODO (29). The final model of native bOBP has R_{work} and R_{free} values of 20.3 and 22.7%, respectively (see Table I), and the final model of the bOBP-AMA complex has R_{work} and R_{free} values of 21.0 and 23.7%, respectively (Table I). The $(F_{obs} - F_{calc})_{exp}(i_{a, calc})$ maps did not show any uninterpretable features. The final models have a good geometry according to the PROCHECK criteria (32), with 91.1% of residues located in the most favorable area, 8.9%

TABLE I
Data collection and final refinement statistics

	bOBP/AMA	bOBP/octenol
Data collection		
Resolution limit (\AA)	18–1.80	55.0–1.80
Data completion ($I/\sigma[I] > 1$) %	92.0	97.8
$I > \sigma[I]$ (all/last shell) ^a	8.5/1.1	5.1/2.5
Redundancy (all/last shell) ^a	2.8/2.8	4.0/3.1
R_{sym} (%; all/last shell) ^a	5.2/40.0	8.2/26.0
Refinement		
Resolution limit (\AA)	10.0–1.80	30.0–1.80
Number of reflections	25530	27094
Number of protein atoms	2582	2582
Number of water molecules	213	150
Final R -factor/ R_{free} %	21.0/23.7	20.3/22.7
B-factors (\AA^2):		
Main chains (molecules A/B)	35.1/28.7	41.6/36.9
Side chains (molecules A/B)	38.4/33.3	45.2/41.3
Solvent/ligands (A/B)	47.8/49.0/49.7	60.3/53.2/52.5
Root mean square deviations from ideal values:		
Bonds (\AA)	0.013	0.008
Angles ($^\circ$)	1.48	1.40
Improper/dihedral angles ($^\circ$)	0.9/25.8	2.1/26.8

^a $R_{sym} = \Sigma (\Sigma |I(h) - \langle I(h) \rangle| / \Sigma \langle I(h) \rangle) / n$; $I(h)$ is the observed intensity of the i -th measurement of reflection h , and $\langle I(h) \rangle$ is the mean intensity of reflection h . Last resolution shell: 1.84–1.80 \AA .

^b $R = \Sigma |F_o - F_c| / \Sigma |F_o|$; F_o and F_c are the observed and calculated structure factor amplitude, respectively.

in additional allowed regions, and no residues in forbidden zones. The coordinates have been deposited in the Protein Data Bank with accession numbers 1G85 (native) and 1HN2 (AMA).

Fluorescence Binding Assay—The fluorescence binding assay of AMA to bOBP and the competition between AMA and 1-octen 3-ol were realized according to the method published by Paolini *et al.* (22), with minor modifications. To avoid interference with the protein absorption band, the excitation wavelength was chosen at 380 nm, where an AMA absorption band is observed, instead of 295 nm (22) or 255 nm (23). The stock solutions of AMA (1–10 mM) in ethanol were preserved in the dark at 4 °C and used within 4 days. The influence of the concentration of ethanol on the chasing process of AMA was tested and found to be negligible up to 1% v/v, a result in contrast with the behavior of rat OBP reported in Briand *et al.* (23). In the case of the direct binding, the titration curves were prepared incubating different samples of bOBP (0.76 μM dissolved in 20 mM Tris-HCl, pH 7.8, 0.5% ethanol (v/v)) with various amounts of AMA ranging from 0.019 to 10 μM for 24 h at 4 °C. In the case of the competition curves, the bOBP samples were incubated with a fixed amount of 2 μM AMA and increasing concentrations of 1-octen-3-ol (0.39–50 μM). Fluorescence emission spectra between 450 and 550 nm were recorded at a fixed excitation wavelength of 380 nm using a PerkinElmer LS 50 luminescence spectrometer, and the formation of the bOBP-AMA complex was detected by the increase of the fluorescence emission intensity at 480 nm. The concentration of the complex was evaluated on the basis of a calibration curve obtained by incubating increasing concentrations of AMA (0.076–5 μM) with a saturating amount of bOBP (10 μM). The binding and competition curves were analyzed using the nonlinear fitting facility of Sigma Plot 5.0 (Cambridge Soft Corp., Cambridge, MA).

RESULTS

Identification of the Ligand—The bOBP organic extract analyzed by gas chromatography yields a prominent peak (Fig. 1A). Comparison of control and native or denatured bOBP showed a single peak difference in mass spectra. After comparison with the Environmental Protection Agency/National Institutes of Health library, the electronic impact mass spectrum of this compound (ions at m/z 41, 43, 55, 57 (100% base pic), 72, 81, 99, 110) was found to correspond to a C8 monoethylenic alcohol (Fig. 1C). This was confirmed with CI/NH₃ data exhibiting ions at m/z 128 and 146 ($(M + NH_4)^+$), leading to a C₈H₁₆O formula. Ions at m/z 57 and 72 (McLafferty rearrangement) in the electronic impact mass spectrum and comparison of the retention times of standards indicated the presence of a secondary alcohol and led us to propose the structure of 1-octen-3-ol (Fig. 1C).

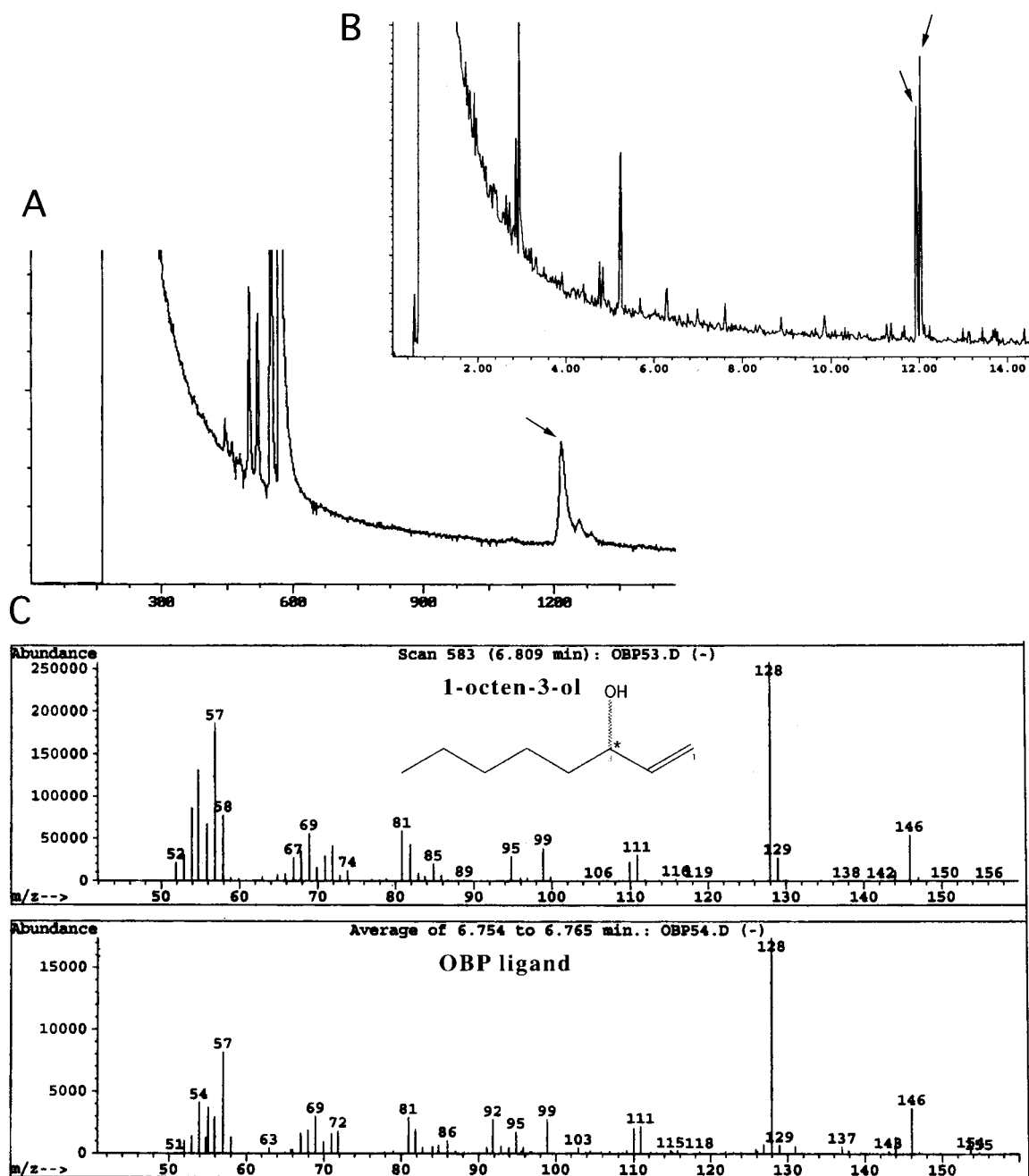


FIG. 1. Gas chromatography-coupled mass spectroscopy of the bOBP extracts. A, chromatogram of the bOBP extract displaying a prominent peak (arrow). B, derivatization of the compound identified in A to identify the presence and quantity of each enantiomer (see "Material and Methods"). C, mass spectra of the main peak identified by gas chromatography in A (bottom) and of the authentic 1-octen-3-ol (top).

Tentative separation of the racemic standard on a chiral gas chromatography column failed. The derivatization of 1-octen-3-ol yielded two peaks in the same gas chromatography conditions (50/50 ratio and electronic impact mass spectra with characteristic ions at m/z 115 and 127 atomic mass units). The derivatization of the natural compound under identical conditions also yielded two peaks with identical mass, retention time, and intensities (Fig. 1B).

Overall Three-dimensional Structure—As described previously, bOBP is a dimer consisting of 2×159 residues at neutral or basic pH and monomerizes at pH values below 4.5 (20). The 2.0-Å resolution structure of bOBP has been reported elsewhere (8). Briefly, each monomer is composed of a lipocalin-type nine-strand β -barrel comprising residues 15–121 (strands 1–8) and residues 145–149 (strand 9) from the other monomer (Fig. 2A). From residue 123 onwards, the topology diverges

from the consensus lipocalin fold. The β -barrel is connected by an extended stretch of residues 123–126 to the α -helix protruding out of the β -barrel and crossing the dimer interface (Fig. 2A). As a consequence, the α -helix of one monomer is placed close to where the α -helix of the other monomer would be if bOBP had a classical lipocalin fold, in a special arrangement called domain swapping (33). In the present structure, the two bOBP polypeptidic chains are visible from residues 1–159 and 3–157 for molecules A and B, respectively.

Internal Cavities and the Buried Ligands—Inside the β -barrel of each monomer, a large buried cavity of about 407 Å³ is observed (Fig. 2A), at a location similar to that observed in other closed lipocalins, such as the major urinary protein (11). Both cavities contain an elongated patch of electron density map, which has been attributed to an 8–10 non-hydrogen atom linear compound in the structure at 2.0-Å resolution (8).

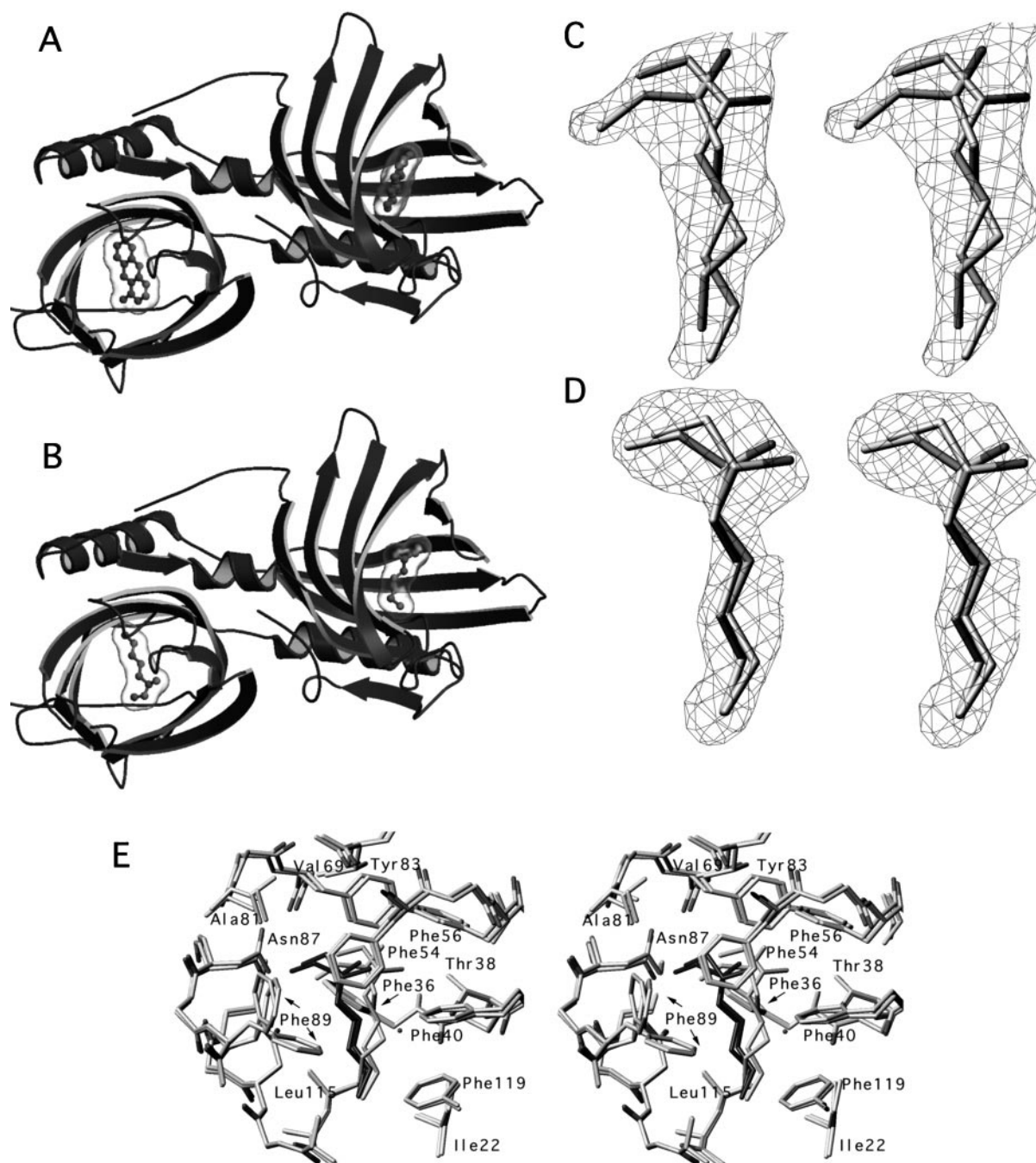


FIG. 2. **The internal ligand binding site of bovine OBP.** A, view of bovine OBP C α trace with the two buried cavities, containing the fluorescent probe AMA and (B) the natural ligand 1-octen-3-ol. C, $2F_o - F_c$ σ_A electron density maps of the racemic 1-octen-3-ol natural ligand in the cavity A of bOBP and (D) in the cavity B. E, stereo view of the superimposed binding cavities A and B with the racemic 1-octen-3-ol natural ligand bound; note the alternative conformations of the ligand and of Phe-89.

Because of the significant improvements in resolution (1.8 Å), data treatment, map calculation, and refinement procedures, interpretable features came out in the difference maps within the buried cavities. Having determined the nature of the ligand by GC/MS, we could fit a molecule of 1-octen-3-ol in each difference electron density map. After CNS refinement, significant patches of electron density still remained in the difference Fourier maps. The two enantiomers of 1-octen-3-ol were then fitted in the most appropriate conformations, and their occupancies were refined in CNS. The resulting structure contains both enantiomers in a ratio close to 1, a result in accord with the GC/MS data (Fig. 2, C and D). In cavity A, the two isomers have very similar orientations and are quasi-superimposed (Fig. 2C). The aliphatic chains of the two isomers are extended

and remain close to each other. The hydroxyl groups point in the same direction, toward an area of the cavity where no hydrogen bond donor is available, however. The positions of the two 1-octen-3-ol enantiomers in the two cavities are slightly different (Fig. 2, C and D), because of a rotation around the ω atom. This movement leaves an empty space in the cavity, between the aliphatic chain of the ligands and the O γ atom of Thr-38, which is filled by a water molecule hydrogen-bonded to the O γ atom (Fig. 2E).

The structure of the bOBP-AMA complex reveals two very well ordered AMA molecules in the buried cavities (Fig. 2A). This indicates clearly that these cavities are the general binding site of bOBP, as in pOBP (6, 13), and discredits the existence of a putative third binding pocket previously proposed (8).

The orientation of AMA in the binding pocket is comparable with that of 1-octen-3-ol, with the long axis perpendicular to the axis of the β -barrel (Fig. 2, A and B).

The walls of these cavities are mostly composed of hydrophobic residues. The water-accessible surface area of bOBP alone or with its ligand was calculated for all the residues. The ligands cover 150 Å² of each cavity surface. Residues Phe-36, Phe-89, Asn-103, Tyr-83, and Phe-54 display the larger loss of surface accessibility upon complexation (10–12 Å²) (Table II). The residues involved in the interaction with the ligand are identical in the two cavities and have similar variation of accessibility. Furthermore, all the residues of both cavities are superimposable, including Phe-89, which is found with two different conformations in each cavity (Fig. 2E).

Fluorescence Binding Assay with AMA and Competition between AMA and 1-Octen-3-ol—The fluorescence properties of AMA when surrounded by a hydrophobic environment have already been used to probe binding in pOBP (20) and porcine salivary OBP (34). We have determined the binding affinity of AMA for ligand-depleted bOBP by titrating at 480 nm the increase in fluorescence signal of AMA upon complexation to the protein (Fig. 3A). The hyperbolic titration curve, with a maximum saturation level of 1.61 molecules of AMA per bOBP molecule, indicates a clear stoichiometry of two AMA molecules per bOBP dimer. The titration of non-extracted bOBP yields a

stoichiometry of 1.85 AMA molecules per bOBP dimer (data not shown), indicating some degradation of bOBP during ligand extraction. The K_d of AMA for bOBP is 1.0 μ M, a value within the range found for most odors toward OBPs (7, 12–16). Because x-ray crystallography experiments indicated that AMA binds in the internal cavities of bOBP described in the previous paragraph, competition of AMA by odors should titrate the same binding site of bOBP, which is the functionally relevant one.

We have determined the binding affinity of 1-octen-3-ol (racemic) by chasing saturating amounts of AMA bound to the internal cavities of bOBP. The decrease of AMA fluorescence at 480 nm was recorded as a function of 1-octen-3-ol concentration (Fig. 3B). The competition curve has a hyperbolic decay with an apparent K_d value of 9.6 μ M. The almost complete displacement of AMA indicates a stoichiometry of two 1-octen-3-ol molecules per bOBP dimer. Taking into account the K_d^{app} of 9.6 μ M, the AMA K_d^{AMA} constant of 1.0 μ M, the AMA concentration of 2 μ M, the Equation 1 below yields a real K_d^{odor} value of 3.3 μ M, for the true dissociation constant of 1-octen-3-ol for OBP. This value indicates that AMA is a better ligand than 1-octen-3-ol for OBP.

$$K_d^{true} = K_d^{app} \times \frac{1}{1 + (1/K_d^{AMA} \times [AMA])} \quad (\text{Eq. 1})$$

TABLE II

Interactions of the natural ligand, the racemic 1-octen-3-ol, with the residues of bOBP internal cavities

The difference in water-accessible surface between free and bound bOBP have been calculated for each residue (Å²).

	Cavity A	Cavity B
Ile-22	8	9
Phe-36	18	21
Thr-38	8	9
Phe-40	11	9
Phe-54	10	11
Phe-56	8	11
Val-69	7	6
Ala-81	4	5
Tyr-83	10	9
Asn-87	7	8
Phe-89	13	17
Ala-101	3	3
Asn-103	17	17
Leu-115	8	8
Thr-116	2	3
Gly-117	2	3
Phe-119	9	9
Total	145	154

DISCUSSION

Identification of lipocalin-bound compounds based on mass spectroscopy coupled to x-ray structure determination has already been successful in the past, for example in the case of the major urinary protein, where four pheromonal components were identified as copurified ligands (11). This procedure failed, however, with aphrodisin, another pheromonal lipocalin (35). In the present study, by using the same type of procedure, we have identified a unique compound, the racemic 1-octen-3-ol, as the naturally occurring copurified ligand of bOBP. Furthermore, both *R* and *S* isomers were found to match nicely the electron density maps of the bOBP natural ligand at 1.8-Å resolution. The contacts between the ligand and amino acid residues of the β -barrel cavities have been characterized at the atomic level. The x-ray structure of the fluorescent probe AMA has revealed that it binds in the same cavity as 1-octen-3-ol. Although several reports of OBP fluorescence titration with AMA are available in the literature, we provide here the first direct evidence that AMA binds in the lipocalin internal pocket. This gives more weight to fluorescence experiments based on ligand displacement, such as those described here. All these

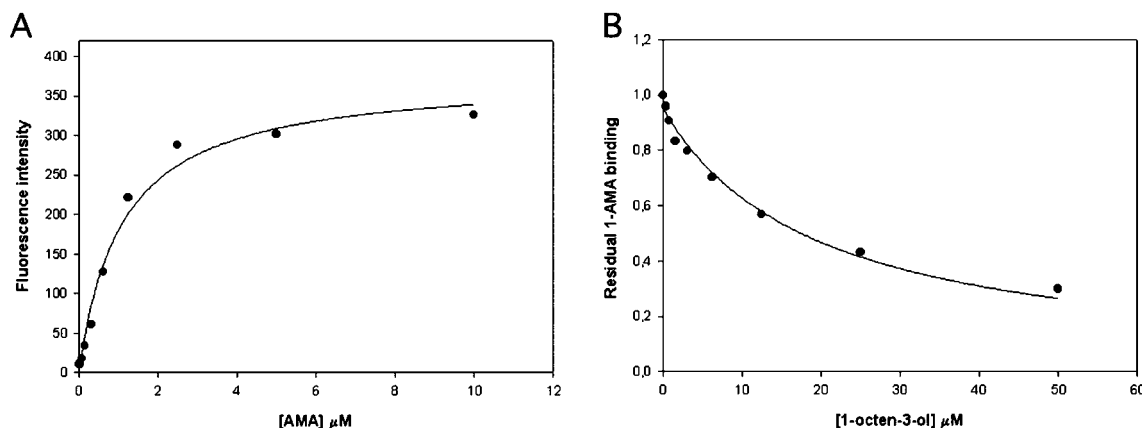


FIG. 3. **Fluorescence titration of the bOBP binding site.** A, fluorescence titration curve of bOBP with AMA. Before the experiment, the natural ligand was removed from the protein by urea denaturation and organic solvent extraction (see “Materials and Methods” for details). B, competition curve between 1-octen-3-ol and AMA on bOBP. The concentration of 1-octen-3-ol is reported *versus* the residual concentration of AMA bound to bOBP (see “Materials and Methods” for details).

results converge to unambiguously identify 1-octen-3-ol (*R,S*) as the natural copurified ligand of bOBP.

Previous studies in solution (1–5) and the recent structural characterization of porcine OBP binding properties (13) have shown that a high degree of hydrophobicity coupled to a molecular mass between 160 and 200 daltons is the main requirement for a ligand to fit the β -barrel cavities of OBP, irrespective of the chemical class, substituents, and molecular structure. These compounds can be odorous chemical messengers that strongly contribute to mediate the relationship between an individual animal and its environment, in food search, mating, etc. (36), or toxic compounds such as natural and synthetic pollutants (19).

Moreover, among all potential ligands of OBPs, two groups can be distinguished: exogenous compounds inhaled from the environment and endogenous compounds produced by the animal. The endogenous compounds can be produced in the nasal mucosa itself as consequence of physiological epithelium turnover, inflammation, and injuries resulting from the action of physical (temperature and humidity), chemical (pollutants and oxidants passing through respiratory airways), and biological (parasites, bacteria, and viruses) aggression. They can also be produced and released by organs (lung, stomach, bloodstream, etc.) and flow through the nasal cavity as breath components. In this context, it is particularly striking to observe that 1-octen-3-ol has an endogenous origin in bovine species and in ruminants in general (37). It is produced in large quantities from fatty acids by lipoxigenases (38) probably associated to the ruminal microflora and then released in the environment as a component of the breath of the animal (37).

It has also been demonstrated that 1-octen-3-ol has a relevant role in the olfactory chemoreception-driven behavior of many worldwide insect species, including parasite vehicles like *Anopheles* and *Glossina* (38, 39). These insects express in their antennae two receptors specific for the breath components 1-octen-3-ol and carbon dioxide, respectively. Their simultaneous stimulation drives host-seeking behavior toward bovines through their breath components (37). The identification of 1-octen-3-ol as the bOBP naturally observed ligand suggests that bOBP might be used by bovines to remove parts of 1-octen-3-ol from the breath flowing through the nasal cavities and to make them less appealing for several insect species. This would result in a general decrease of the number of insect bites and furthermore might partially protect the animal from parasitosis and infectious diseases carried by these insect vectors.

This hypothesis on the possible role of OBP in the ecological relationships between bovine and insect species must be limited, at present, to the case of bovine species, because only in this case has the presence and the role of the breath component 1-octen-3-ol in the ecological relationships with insects been extensively documented. Besides, this function should not be taken as an alternative to the other roles previously proposed, such as that of a binder of exogenous compounds. All the possible putative roles of OBPs in mammalian physiology, toward either endogenous or exogenous compounds, are compatible with their above-mentioned capacity to bind several classes

of small molecules, with their stability, and with their abundant production and presence in nasal mucosa.

REFERENCES

- Pelosi, P. (1994) *Crit. Rev. Biochem. Mol. Biol.* **29**, 199–228
- Pelosi, P. (1995) *J. Neurobiol.* **30**, 3–19
- Pelosi, P., Baldaccini, N. E., and Pisanelli, A. M. (1982) *Biochem. J.* **201**, 245–248
- Cavaggioni, A., Sorbi, R. T., Keen, J. N., Pappin, D. J. C., and Findlay, J. B. C. (1987) *FEBS Lett.* **212**, 225–228
- Bignetti, E., Cavaggioni, A., Pelosi, P., Persaud, K. C., Sorbi, R. T., and Tirindelli, R. (1985) *Eur. J. Biochem.* **149**, 227–231
- Tegoni, M., Pelosi, P., Vincent, F., Spinelli, S., Campanacci, V., Grolli, S., Ramoni, R., and Cambillau, C. (2000) *Biochim. Biophys. Acta* **1482**, 229–240
- Flower, D. R. (1996) *Biochem. J.* **318**, 1–14
- Tegoni, M., Ramoni, R., Bignetti, E., Spinelli, S., and Cambillau, C. (1996) *Nat. Struct. Biol.* **3**, 863–867
- Bianchet, M. A., Bains, G., Pelosi, P., Pevsner, J., Snyder, S. H., Monaco, H. L., and Anzel, L. M. (1996) *Nat. Struct. Biol.* **3**, 934–939
- Cowan, S. W., Newcomer, M. E., and Jones, T. A. (1990) *Proteins* **8**, 44–61
- Böcskei, Z., Groom, C. R., Flower, D. R., Wright, C. E., Phillips, S. E. V., Cavaggioni, A., Findlay, J. B. C., and North, A. C. T. (1992) *Nature* **360**, 186–188
- Spinelli, S., Ramoni, R., Grolli, S., Bonicel, J., Cambillau, C., and Tegoni, M. (1998) *Biochemistry* **37**, 7913–7918
- Vincent, F., Spinelli, S., Ramoni, R., Grolli, S., Pelosi, P., Cambillau, C., and Tegoni, M. (2000) *J. Mol. Biol.* **300**, 127–139
- Eckl, P., Ortner, A., and Esterbauer, H. (1995) *Mutat. Res.* **290**, 183–192
- Pelosi, P., and Tirindelli, R. (1989) in *Chemical Senses* (Brand, J. G., Teeter, J. H., Cagan, R. H., and Kare, M. R., eds) Vol. 1, pp. 207–226, Marcel Dekker, Inc., New York
- Pevsner, J., Sklar, P. B., Hwang, P. M., and Snyder, S. H. (1989) in *Chemical Senses* (Brant, J. G., Teeter, J. H., Cagan, R. H., and Kare, M. R., eds) Vol. 1, pp. 227–242, Marcel Dekker, Inc., New York
- Dal Monte, M., Centini, M., Anselmi, C., and Pelosi, P. (1993) *Chem. Senses* **18**, 713–721
- Hérent, M.-F., Collin, S., and Pelosi, P. (1995) *Chem. Senses* **20**, 601–608
- Boudjelal, M., Sivaprasadarao, A., and Findlay, J. B. C. (1996) *Biochem. J.* **317**, 23–27
- Bignetti, E., Damiani, G., De Negri, P., Ramoni, R., Avanzini, F., Ferrari, G., and Rossi, G. L. (1987) *Chem. Senses* **12**, 601–608
- Patel, R. C., Lange, D., McConathy, J. M., Patel, Y. C., and Patel, S. C. (1997) *Protein Eng.* **10**, 621–625
- Paolini, S., Tanfani, F., Fini, C., Bertoli, E., and Pelosi, P. (1999) *Biochim. Biophys. Acta* **1431**, 179–188
- Briand, L., Nespoulos, C., Perez, V., Rémy, J.-J., Huet, J.-C., and Pernellet, J.-C. (2000) *Eur. J. Biochem.* **267**, 3079–3089
- Edelhoc, H. (1967) *Biochemistry* **22**, 1948–1954
- Pace, C. N., Vajdos, F., Fee, L., Grimsley, G., and Gray, T. (1995) *Protein Sci.* **4**, 2411–2423
- Slessor, K. N., King, C. C. S., Miller, D. R., Winston, M. L., and Cutforth, T. L. (1985) *J. Chem. Ecol.* **11**, 1659–1667
- Otwinovski, Z. (1993) in *Data Collection and Processing* (Sawyer, L., Isaacs, N. W., and Bailey, S., eds) pp. 56–63, DLSCI/R34 Daresbury Laboratory, Warrington, United Kingdom
- Collaborative Computing Project 4 (1994) *Acta Crystallogr. Sect. D Biol. Crystallogr.* **50**, 760–766
- Roussel, A., and Cambillau, C. (1991) in *Silicon Graphics Geometry Partners Directory*, p. 81, Mountain View, CA
- Brunger, A. T., Adams, P. D., Clore, G. M., DeLano, W. L., Gros, P., Grosse-Kunstleve, R. W., Jiang, J.-S., Kuszewski, J., Nilges, M., Pannu, N. S., Read, R. J., Rice, L. M., Simonson, T., and Warren, G. L. (1997) *Crystallographic and NMR System (CNS)*, CNS Solve, Yale University Press, New Haven, Connecticut
- Read, R. J. (1986) *Acta Crystallogr. Sect. A* **42**, 140–149
- Laskowski, R., MacArthur, M., Moss, D., and Thornton, J. (1993) *J. Appl. Crystallogr.* **26**, 91–97
- Bennet, J. M., Schlunegger, M. P., and Eisenberg, D. (1995) *Protein Sci.* **4**, 2455–2468
- Loebel, D., Scaloni, A., Paolini, A., Fini, C., Ferrara, L., Breer, H., and Pelosi, P. (2000) *Biochem. J.* **350**, 369–379
- Vincent, F., Löbel, D., Brown, K., Spinelli, S., Grote, P., Breer, H., Cambillau, C., and Tegoni, M. (2001) *J. Mol. Biol.* **305**, 459–469
- Krieger, J., and Breer, H. (1999) *Science* **286**, 720–723
- Takken, W., and Knols, B. G. J. (1999) *Annu. Rev. Entomol.* **44**, 131–157
- Husson, F., Couturier, A., Kermasha, S., and Belin, J. M. (1998) *J. Mol. Catal. B Enzym.* **5**, 159–163
- van den Broek, I. V. F., and den Otter, C. J. (1999) *J. Insect Physiol.* **45**, 1001–1010